Bio-Design and Manufacturing (2020) 3:60–70
https://doi.org/10.1007/s42242-020-00059-7

RESEARCH ARTICLE

Guided cell migration on a graded micropillar substrate

Srikumar Krishnamoorthy[1] · Zhengyi Zhang[2] · Changxue Xu[1]

Received: 19 December 2019 / Accepted: 16 January 2020 / Published online: 24 January 2020

Abstract
Cell migration is facilitated by the interaction of living cells and their local microenvironment. The local topography is one of the key factors regulating cell migration. Interaction between the surface topography and the cell behaviors is critical to understanding tissue development and regeneration. In this study, a dynamic mask photolithography technique has been utilized to fabricate a surface with graded micropillars. It has been demonstrated that the cells have been successfully guided to migrate from the sparse zone to the dense zone. The cell polarization angle has been characterized in both sparse zone and the dense zone. Compared to the dense zone, the cells in the sparse zone are more aligned along the direction of the micropillar spacing gradient, which enables the guided cell migration. Moreover, the effects of the micropillar spacing gradient, micropillar diameter, and micropillar height have been investigated in terms of the cell migration speed and cell spreading area. Finally, two issues significantly affecting the cell migration have been discussed: trapped cells between the micropillars and cell clusters.

Keywords Guided cell migration · Graded microtopography · Cell polarization

Introduction

Guided cell migration refers to the tailoring of local cell environment to guide cell movement in preferred ways [1]. Guided cell migration has a variety of potential applications in cell sorting [2], wound healing [3, 4], diagnosis of infections [5], and treatment of strokes and other brain injuries [6]. For example, pre-stalk and pre-spore spells of *Dictyostelium discoideum* can be sorted from an initially mixed population by utilizing the different migration responses of the cells toward various chemoattractants [2], which benefits the replication of a wide range of complex natural biological processes in the laboratory, such as embryogenesis and organ growth [2]. Wound healing can be enhanced by the use of chemoattractants to guide fibroblasts to fill wounds and blisters [3, 4]. The diagnosis of infections has been performed by assessing the migratory response of human neutrophils from a patient with recurrent bacterial infections on a soft microdevice [5]. Human neural stem cells have been guided using electric fields to migrate to specific locations, which could be utilized in the human brain to facilitate the treatment of strokes and other brain injuries [6].

The active migration of cells occurs due to the interaction between the actin cytoskeleton of the cell and local environmental cues. Mainly, cells possess actin-rich protrusions on the plasma membrane, namely filopodia and lamellipodia, which can function as antennae for cells to sense the local environment [7]. Filopodia are commonly found embedded within or protruding from the lamellipodia at the free front of migratory tissue sheets. During cell migration, the filopodia are localized at the leading cell edge and probe the microenvironment based on the mechanism of contact-angle sensing [8]. The local environmental cues allow the cells to align in specific directions, known as cell polarization [9, 10]. Depending on different environmental cues, there have been several cell migration mechanisms identified in the literature. Haptotaxis is a directional cell movement in response to immobile chemical signals [11]. Durotaxis is a directional cell movement guided by rigidity gradients [12]. Galvanotaxis utilizes electrical signals to guide cell migration [13]. Recently, a new mechanism has been proposed for

✉ Changxue Xu
changxue.xu@ttu.edu

[1] Department of Industrial, Manufacturing, and Systems Engineering, Texas Tech University, Lubbock, TX 79409, USA

[2] School of Naval Architecture and Ocean Engineering, Huazhong University of Science and Technology, Wuhan 430074, China

guided cell migration, namely topotaxis, which refers to the cell migration caused by the response of cells to the local topographic environment.

The filopodia of cells can sense the area of cell contact and direct the cells to the optimal zone with a greater contact area. Cell migration due to topotaxis is based on the mechanism that the cells try to maximize their contact surfaces with the surrounding topography, which are determined by the relative stiffness of cells and the local topographic environment. When cells are stiffer than its surrounding architecture, there is limited penetration into the surrounding matrix, which can limit the contact between the cell and the surrounding topography. The cells will be guided from the sparse fiber zone to the dense fiber zone, so that the cells can have greater contact areas with the surrounding matrix. When cells are softer than its surrounding architecture, they can penetrate into the inter-fiber spaces. The cells will migrate from the sparse fiber zone to the dense fiber zone, which increases their contact area with the surrounding matrix. If the stiffness of cells is intermediate compared to the surrounding architecture, the cells can penetrate into the sparse fiber zone due to large inter-fiber spaces, but the cells cannot penetrate into the dense fiber zone due to narrow inter-fiber spaces. The cells will migrate from the dense fiber zone to the sparse fiber [14]. The principle of topography sensing in the migration of cells has been documented in the literature. For instance, Kim et al. [15] demonstrated that anisotropic nanotopographic surface gradients were shown to influence the cell shape and movement of 3T3 fibroblasts. Specifically, it was observed that along sparse gradients of a graded nanogroove surface, cells tended to orient themselves randomly similar to cells adhered on flat non-graded surfaces, while on dense gradients, cells were shown to elongate longer along the direction of the grooves. Park et al. [16] demonstrated the directed migration of melanoma cells on graded nanopillars arrays. It was reported that invasive and noninvasive cancer cells exhibited the migration in opposite directions, as a result of the differences in their relative stiffness. Hui et al. [17] investigated the migration of MC3T3-E1 osteoblast cells with response to micropillars and noted that an increase in spacing between micropillars resulted in a significant increase in the migration speed of the cells. Wei et al. [18] fabricated micropillars of different heights to study the interaction of 3T3 cells with them and reported that cells were sensitive to the height of the micropillars and tended to preferentially localize in the stiffer regions on the substrate. Alapan et al. [19] demonstrated the effect of anisotropically stiff micropillars on cell morphology and elongation and reported the preferential elongation of cells along the stiffer areas.

Cell migration in response to local topographic environment is a complex interaction between the cells and the surrounding microenvironment. Prior research has primarily focused on the underlying migration mechanism of cells on nanoscale structures. However, the interaction between cells and microscale structures and the potential applications have not been explored in detail. The objective of this paper is to investigate the effects of the topographic parameters on the cell migration speed and cell spreading area and demonstrate a possible application, namely guided cell migration. There are several critical parameters which may significantly influence the cell migration on a graded micropillar substrate, including the micropillar diameter, height, and spacing gradient. This paper is organized in the following manner. First, the experimental materials and methods are introduced in detail. Second, the overall cell migration on a graded micropillar substrate is demonstrated. Third, the effects of topographic parameters on the cell migration speed and cell spreading area are studied. Finally, the major conclusions are listed, and future work is proposed.

Materials and methods

Micropillar substrate fabrication

There are primarily three types of topographic features that can be used to mimic natural ECM structures, namely posts, pits, and grooves [20]. The micropost arrays are specifically sensitive to the contractility of cells, and the substrate stiffness can be easily tailored by modifying the diameter, height, and/or spacing between posts [21]. Moreover, the use of a silicone elastomer as the substrate allows for the controlling of the surface rigidity, which influences the cell migration, as demonstrated in the reported studies [17]. Microscale topographic patterns were designed as binary image files and digitally inverted in order to use in the lithographic process and maintain compatibility with the negative photoresist.

The fabrication of the graded micropillar substrate is shown in Fig. 1. Initially, a silicon master was fabricated using a maskless lithographic technique (Durham Magneto Optics ML3, Durham, UK). Then, the pattern was transferred to a polydimethylsiloxane (PDMS) substrate. Finally, the topographic substrate was subject to a two-step surface treatment (plasma processing and coating with gelatin) to facilitate cell attachment onto the fabricated micropillar substrate. To fabricate the silicon master, a negative photoresist (HARE SQ-10, KemLab, Woburn, MA) was evenly coated on a silicon wafer (University Wafer, Boston, MA) using a spin coater (KW-4A, Chemat Technology, Northridge, CA). Then, the coated silicon wafer was baked at 65 °C for 3 min and 95 °C for 5 min. The coated wafer was subject to a UV exposure with the graded micropillar pattern, the UV wavelength was 385 nm, and the intensity was 500 mW/cm^2. This

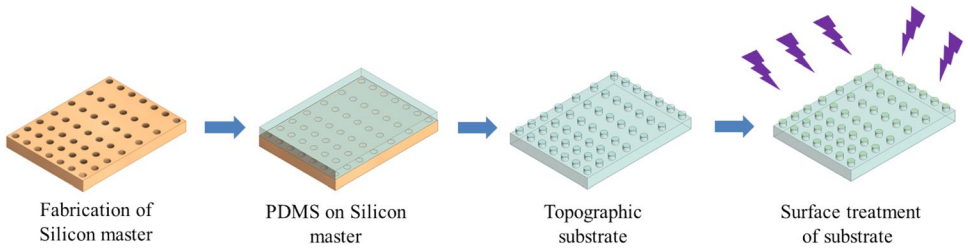

Fig. 1 Schematic of micropillar substrate fabrication

was followed by a post-exposure baking process at 65 °C for 3 min and 95 °C for 5 min and development with a chemical developer (HARE SQ Developer, KemLab, Woburn, MA) for 2.5 min. The transferring of the pattern to the silicone elastomer substrate was performed by using a capillary molding technique. PDMS (Sylgard 184, Dow Corning, Midland, MI) was utilized to fill the cavity of the pattern on the silicon master. The PDMS micropatterns were formed after cross-linking PDMS at 65 °C for 4 h.

In order to facilitate cell seeding and attachment, the micropatterns were subject to a two-step surface treatment shown in Fig. 2. The first step is exposing the PDMS patterns to plasma via corona discharge (BD-20, Electro-Technic Products, Chicago, IL) for 40 s. During the plasma processing, the methyl groups were replaced by the hydroxyl groups, resulting in hydrophilic properties of the micropatterns [22]. The second step is coating a single layer of gelatin. Gelatin is a partial derivative of collagen and has properties that promote cell adhesion, migration, and proliferation [23]. The micropatterns were covered with a 0.5% (w/v) type-A gelatin solution in Dulbecco's phosphate-buffered saline (DPBS) for 3 h, which bound the amine group from gelatin onto the hydroxyl groups of the plasma-treated PDMS [24]. The residual gelatin was washed away using DPBS to ensure a uniform coating of gelatin on the micropatterns.

Cell culture and seeding

Fibroblasts are the most common type of cells found in connective tissues of animals and have been widely utilized in a variety of applications in 3D bioprinting [25, 26], regenerative medicine [27], and cell migration [28, 29]. In this study, fibroblasts were used as the model cells. NIH 3T3 mouse fibroblasts (ATCC, Rockville, MD) were cultured using Dulbecco's modified Eagles medium (DMEM; Sigma-Aldrich, St. Louis, MO) supplemented with 1% antibiotic/antimycotic solution (Corning, Manassas, VA) and 10% fetal bovine serum (FBS; HyClone, Logan, UT) inside a humidified 5% CO_2 incubator at 37 °C. The culture medium was replaced every 3 days as required. Prior to usage, cells were detached from the culture flasks by the addition of 0.25% trypsin/EDTA (Sigma-Aldrich, St. Louis, MO) at 37 °C for 3 min [30]. The cell suspension was centrifuged at 1000 rpm for 5 min, and the resulting cell pellet was resuspended in the cell culture medium to make the bioink with a cell concentration of 1×10^5 cells/ml.

The bioink was added on the fabricated micropillar substrate followed by a six-hour incubation at 37 °C for the cell attachment. After the cell attachment, images were taken every 2 h for a total of 6 h. At each point of observation, the relative position and the surface area of the cells were measured using the software ImageJ developed by the National Institutes of Health. The cell migration speed was calculated based on the cell migration distance divided by the time.

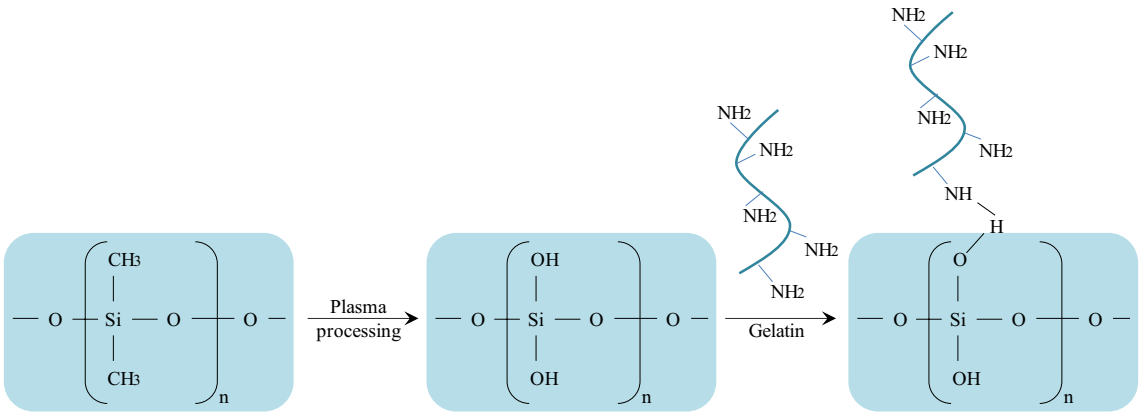

Fig. 2 Two-step surface treatment of PDMS micropatterns to facilitate cell seeding and attachment: plasma processing and coating of gelatin

Cell migration distance was defined as the distance between the tips of the cells. Cell migration speed is characterized as the average speed within 2 h at each point of observation.

Experimental conditions and design

There are several critical parameters which may significantly influence the cell migration on the graded micropillar substrate, including the diameter of the micropillars, height of the micropillars, and the spacing gradient. In this paper, the effects of the micropillar diameter, height, and spacing gradient on the cell migration speed and cell spreading area have been investigated. The detailed experimental conditions and design are micropillar diameters of 4 μm, 6 μm, and 8 μm, spacing gradients of 0.1 μm, 0.2 μm, and 0.3 μm, and micropillar heights of 10 μm, 20 μm, and 30 μm.

Moreover, the lateral direction of the micropillars is defined as the direction with evenly spaced micropillars. The longitudinal direction of the micropillars is defined as the direction where the space between adjacent micropillars is subsequently increased by a distance equal to the spacing gradient. For instance, along the longitudinal direction, the minimum spacing between the adjacent rows of micropillars is 2 μm, and each row is increased by the spacing gradient, with the maximum spacing between the adjacent rows of micropillars being 14 μm. When investigating the effects of the topographic parameters on the cellular morphology on the graded micropillar substrate, each condition had three replicates and was repeated three times. Each experimental condition was analyzed separately, after fixing the other conditions, and one-way ANOVA was used to perform statistical analyses.

For the demonstration of guided cell migration, the diameter of the micropillars used is 8 μm, and the spacing gradient used is 0.1 μm. The bioink was added on the fabricated micropillar substrate followed by incubation for six hours at 37 °C for the cell attachment. In order to better visualize the cell attachment, fluorescent dyes were utilized to stain the cell membrane and nucleus. The cells were fixed and permealized using 4% formaldehyde (Santa Cruz Biotechnology Inc., Dallas, TX), followed by staining of the membrane with phalloidin (Santa Cruz Biotechnology Inc., Dallas, TX), and staining of the nucleus with 4′-6-diamidino-2-phenylindole (DAPI) (Santa Cruz Biotechnology Inc., Dallas, TX). Imaging was performed using a fluorescent microscope (EVOS FL, Thermo Fisher Scientific, Waltham, MA). After the fibroblasts were seeded on the graded micropillar substrate, substrates were randomly chosen every 6 h, and imaging was performed periodically over 12 h, after permeabilization of the cells. To facilitate quantification of bulk cell migration, the graded micropillar substrate was divided into two equal halves, namely the sparse and dense zones. The number of cells in each zone was counted using the ImageJ [31]. The experiments were repeated three times.

Results

When cells attach on the top of a microtopographic array, they spread their contact area over multiple micropillars. In this study, the graded micropillar substrate is utilized with a spacing gradient between the micropillars. This graded micropillar substrate can be considered as a substrate with a stiffness gradient which can be sensed by the cells and guide the cell migration. The effective stiffness at the specific location of the micropillar substrate can be calculated based on the spring constant of a single micropillar and the number of micropillars under a cell. The spring constant of a single micropillar can be calculated using the following formula [32, 33]:

$$k = \frac{3}{4}\pi \cdot E \cdot \frac{r^4}{H^3} \tag{1}$$

where E is the Young's modulus of the material, r is the radius of the micropillar, and H is the height of the micropillar. Since the cell spreads over multiple micropillars, the effective spring constant at the specific location is $k_{\text{eff}} = n \cdot k$ where n is the number of micropillars under a cell [32]. The effective Young's modulus at the specific location of the micropillar substrate is obtained as [18, 33]:

$$E_{\text{eff}} = \frac{9 \cdot k_{\text{eff}}}{4 \cdot \pi \cdot r} \tag{2}$$

A perfectly flat substrate is considered to have a Young's modulus of the material, namely PDMS in this study. When the micropillars are present, the effective Young's modulus of the substrate is reduced. The spacing between the micropillars can be large or small, resulting in a relatively sparse zone or dense zone. In the sparse zone, the effective Young's modulus is lower, while in the dense zone, the effective Young's modulus is higher. This differential stiffness is considered as the primary reason for the cell migration due to topotaxis [16]. Cell migration is a dynamic process that incorporates continuous cell adhesion and detachment on a surface [34]. Typically, the four main steps involved in cell migration are the protrusion of the leading edge of the cell in the direction of movement, adhesion to the ECM, shifting of the cellular body in the direction of the movement, and the corresponding retraction of the trailing edge of the cell [35].

Demonstration of guided cell migration on a micropillar substrate

The schematic of a fabricated graded micropillar substrate is shown in Fig. 3. It also shows the fluorescent image of cells attached successfully on the substrate.

The results of fluorescent imaging performed at 0 h, 6 h, and 12 h are shown in Fig. 4. The substrate in Fig. 4 is divided into the sparse zone and dense zone in order to facilitate better visualization of bulk cell migration. There is no physical interface between the sparse zone and the dense zone. It is seen that at 0 h, the cells were seeded evenly on the graded micropillar substrate. With the incubation time, a greater number of cells are shown to be attached on the dense zone where compared to the sparse zone, which indicates the migration of cells from the sparse zone to the dense zone. In Fig. 5, the percentage of cells in the sparse and dense zone with the incubation time is shown. At 0 h, the average percentage of the cells in the sparse zone and dense zone is 52% and 48%, respectively. This represents the almost even distribution of the cells attached on the substrate. After 6 h, the average percentage of the cells in the dense zone is 66%, which is much higher than that in the sparse zone. After 12 h, over 85% cells in average migrate to the dense zone. In this case, the cell migration is due to a topographic gradient, and the direction of the movement is determined by the micropillar spacing gradient of the substrate. The fibroblasts are directed to migrate from the sparse zone to the dense zone.

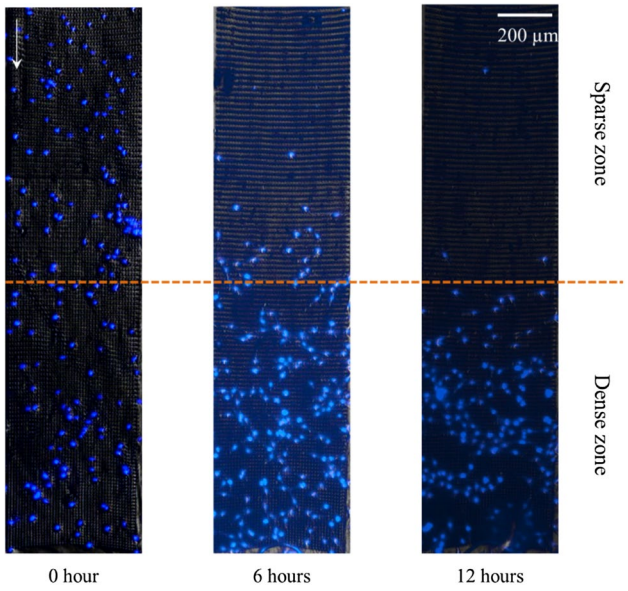

Fig. 4 Demonstration of the cell migration from the sparse zone to dense zone on the graded micropillar substrate. The graded micropillar substrate has a micropillar diameter of 8 μm, micropillar height of 30 μm, and spacing gradient of 0.1 μm. The green color represents the stained cell membranes, and the blue color represents the stained cell nuclei

Cell polarization on a graded micropillar substrate

This section focuses on the cell polarization angle during the guided cell migration on the graded micropillar substrate. The graded micropillar substrate has the micropillar diameter of 8 μm and a spacing gradient of 0.1 μm. The cell polarization angle was quantified by the acute angle between the major axis of the cell (direction of maximal elongation) and the lateral direction of the micropillars. When the cells align perfectly along the lateral direction of the micropillars, the polarization angle is 0°. When the cells align perfectly along the longitudinal direction of the micropillars, the polarization angle is 90°. Figure 6 shows representative florescent images of cells attached in the sparse zone and dense zone. It is seen that the polarization angles of the cells in the sparse zone are larger than the ones of the cells in the dense zone. Consequently, cells in the dense zone are more oriented along the longitudinal direction of the micropillars,

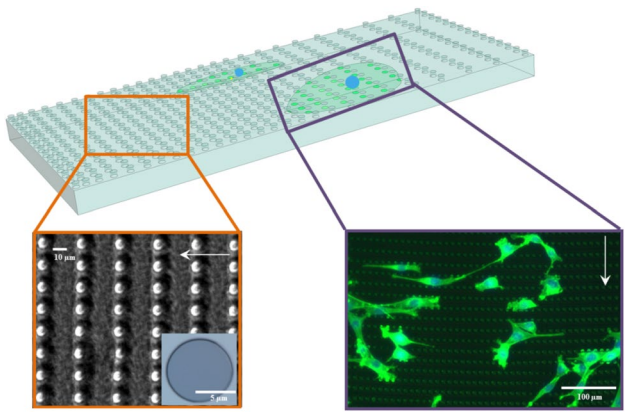

Fig. 3 Schematic of the graded micropillar substrate with zoom-in individual micropillars and fluorescent image of attached cells. The arrows indicate the direction from the sparse zone to the dense zone. The graded micropillar substrate has a micropillar diameter of 8 μm, micropillar height of 30 μm, and spacing gradient of 0.1 μm. The green color represents the stained cell membranes, and the blue color represents the stained cell nuclei

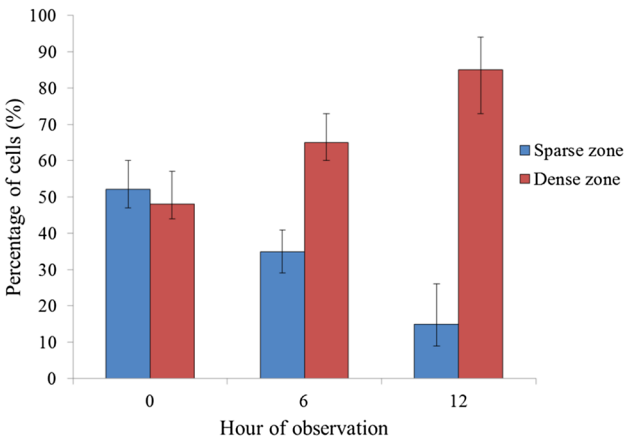

Fig. 5 Percentage of cells remaining on the sparse and dense zones at different hours of observation

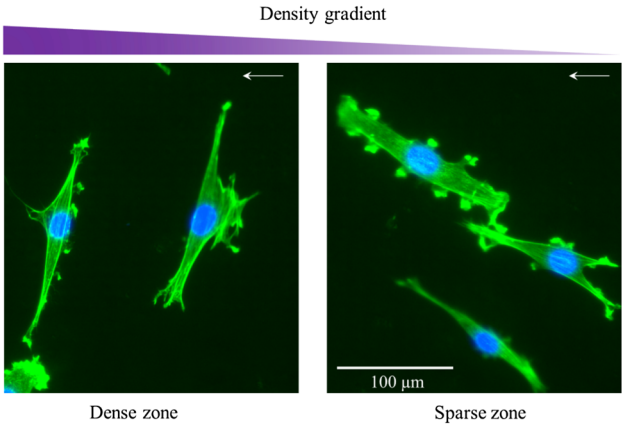

Fig. 6 Representative images of the cells in the sparse zone and dense zone. The arrows indicate direction along the gradient from sparse zone to the dense zone. The graded micropillar substrate has a micropillar diameter of 8 μm, micropillar height of 30 μm, and spacing gradient of 0.1 μm. The green color represents the stained cell membranes, and the blue color represents the stained cell nuclei

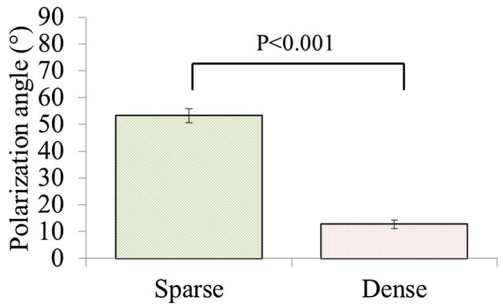

Fig. 7 Cell polarization angle in the sparse zone and dense zone

which is the direction of the micropillar spacing gradient. It indicates that the cells can sense and respond to the variation in the local topography on the level of the microscale.

In order to quantify the cell polarization angle in different topographic zones, 50 cells were randomly selected to measure the angle in both sparse zone and dense zone. In Fig. 7, it is seen that the graded microtopographic substrate significantly affects the cell polarization angle. In the dense zone, the average polarization angle is only 13°, while the average polarization angle is 53° in the sparse zone. The cells in the sparse zone are more aligned along the longitudinal direction of the micropillars, which enables the guided migration of cells along the micropillar spacing gradient toward the denser topographic area. On the contrary, the cells in the dense zone are oriented along the lateral direction of micropillars, which is the direction of the micropillars without any topographic gradient and can impair their subsequent migration in the direction of the micropillar spacing gradient. This observation is consistent with the reported results using the micro- and nanostructured ridge/groove pattern arrays [15]. Figure 8 shows the distribution of cell polarization angles in the sparse zone and dense zone after six hours of migration. It is observed that the distribution of cell polarization angles in the sparse zone is skewed toward higher angular values above 40°, while the cells in the dense zone have majority of the cells with much lower polarization angles. The overall percentage of the cells in the dense zone that are migrating along the micropillar spacing gradient (longitudinal direction) is much lower than the overall percentage of the cells in the sparse zone that are migrating along the gradient, which is also confirmed by the bulk cell migration demonstration experiments. These observations show that the gradient direction influences cell polarization, which plays an important role in guided cell migration of attached cells from the sparse zone to the dense zone.

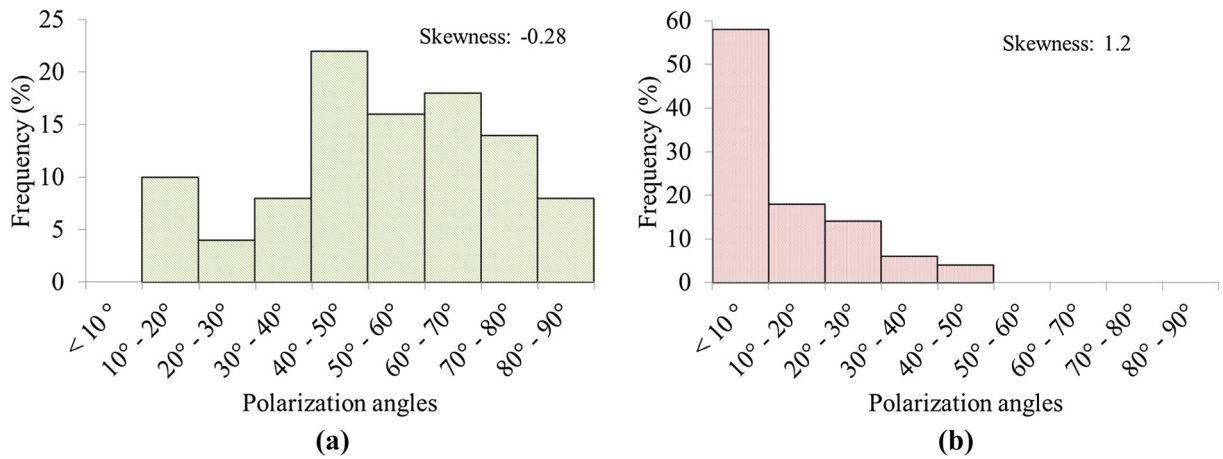

Fig. 8 Distribution of cell polarization angles in **a** sparse zone, and **b** dense zone after 6 h of migration

Effects of topographic parameters on cell migration

There are several critical parameters which may significantly influence the cell migration on a graded micropillar substrate, including the diameter of the micropillars, height of the micropillars, and the spacing gradient. In this section, the effects of these three topographic parameters have been investigated in terms of the cell migration speed and spreading area. Fibroblasts were seeded on the graded micropillar substrate by dispensing 0.1 ml bioink with a cell concentration of 12,500 cells/ml. The cells were allowed to adhere to the substrate for 6 h and migrate on the substrate for 6 h, similar to other studies [17, 18]. The measured average cell migration speed under different conditions is in the range of 4–27 μm/h, which is comparable to the reported migration speed of fibroblasts [12, 36]. The measured average cell spreading area is in the range of 736–906 μm^2, which is also comparable to the spreading areas of fibroblasts of 500–1800 μm^2 on a flat surface with a varying stiffness [33]. The maximum observed cell spreading area in this study is 906 μm^2, which is much less than 1800 μm^2 reported on a flat surface [33]. This is mainly due to the micropillars patterned on the substrate confining the cell attachment and spreading.

In Fig. 9, it shows the effects of the three topographic parameters on the cell migration speed. For the cells in the sparse zone, it is seen that as the micropillar spacing gradient increases from 0.1 to 0.2 to 0.3 μm, the cell migration speed decreases notably from 23.5 to 17.9 to 14.5 μm/h. The *P* value is demonstrated to be less than an alpha value of 0.1, which indicates that the spacing gradient may have a moderate effect on the cell migration speed in the sparse zone. In addition, with the increase in the micropillar diameter, the cell migration speed in the sparse zone increases significantly. At the micropillar diameter of 4 μm, the cell migration speed is 7.6 μm/h, while for the micropillar diameter of 8 μm, the cell migration speed increases to 23.5 μm/h. The *P* value is less than 0.05, which indicates that the micropillar diameter has a demonstrably significant effect on the cell migration speed. With the increase in the micropillar height, the cell migration speed in the sparse zone is observed to have no significant change. At the micropillar height of 10 μm, the cell migration speed is 24 μm/h; at the micropillar height of 20 μm, the cell migration speed is 24.6 μm/h; and at the micropillar height of 30 μm, the cell migration speed is 23.5 μm/h. For the cells in the dense zone, the cell migration speed generally has no significant change under different topographic parameters. In Fig. 9, it is also seen that the three topographic parameters have no significant effects on the cell spreading area in both sparse zone and dense zone. However, the micropillar densities in the two zones are different. The micropillars are much closer with each other in the dense zone. Hence, the contact area of the cells in the dense zone is much larger than that in the sparse zone. The cells migrate from the sparse zone to the dense zone, which indicates that the filopodia of cells can sense the area of cell contact and direct the cells to the optimal zone with a greater contact area.

In Fig. 9, it is seen that the cell migration speed in the sparse zone is generally significantly greater than that in the dense zone. For example, in Fig. 9a at the micropillar spacing gradient of 0.1 μm the cell migration speed in the sparse zone is 23.5 μm/h, while it is only 9.3 μm/h in the dense zone. In Fig. 9c, at different micropillar heights the cell migration speed in the spare zone is around 24–25 μm/h compared to the cell migration speed of 7–9 μm/h in the dense zone. Cell migration is a complex cell–ECM interaction determined by the relative stiffness of cells and the local ECM topographic environment. The cells migrate in order to optimally increase their contact area with the substrate [16]. The mechanism of the cell migration is that the cells can sense the local topographic environment through the actin fibers and realign themselves to migrate toward a more optimal zone through the protrusion and retraction of the leading and trailing edges [37]. The cell migration is a result of repeated cell adhesion and detachment which is simultaneously coupled with an increase in their spreading area on the substrate [35]. Compared to the sparse zone, the dense zone generally has a greater cell contact area due to the closer micropillars and can provide more functional adhesion sites for the cells. Hence, the cellular migration speed decreases with the increase in the cell contact area, as observed in the prior literature [38].

Discussion

This study investigates the guided cell migration on the graded micropillar substrate. The cells attached on the substrate can sense the area of cell contact and migrate to the optimal zone with a greater contact area. Typically, the four main steps involved in cell migration are the protrusion of the leading edge of the cell in the direction of movement, adhesion to the ECM, shifting of the cellular body in the direction of the movement, and the corresponding retraction of the trailing edge of the cell [35]. For the cellular adhesion step, cells require a minimum functional adhesion area. For fibroblasts, each focal adhesion point on a flat surface has been estimated to be around 3 μm [33], which indicates the physiological limit for fibroblasts to attach. In this study, the fibroblasts are seeded on the graded micropillar substrate. The fibroblasts contact with the micropillar array and stay on the top of the micropillar array. The micropillar diameters used in this study are 4, 6, and 8 μm, which are larger than the physiological limit for fibroblasts to attach on the surface. If the micropillar diameter is small enough,

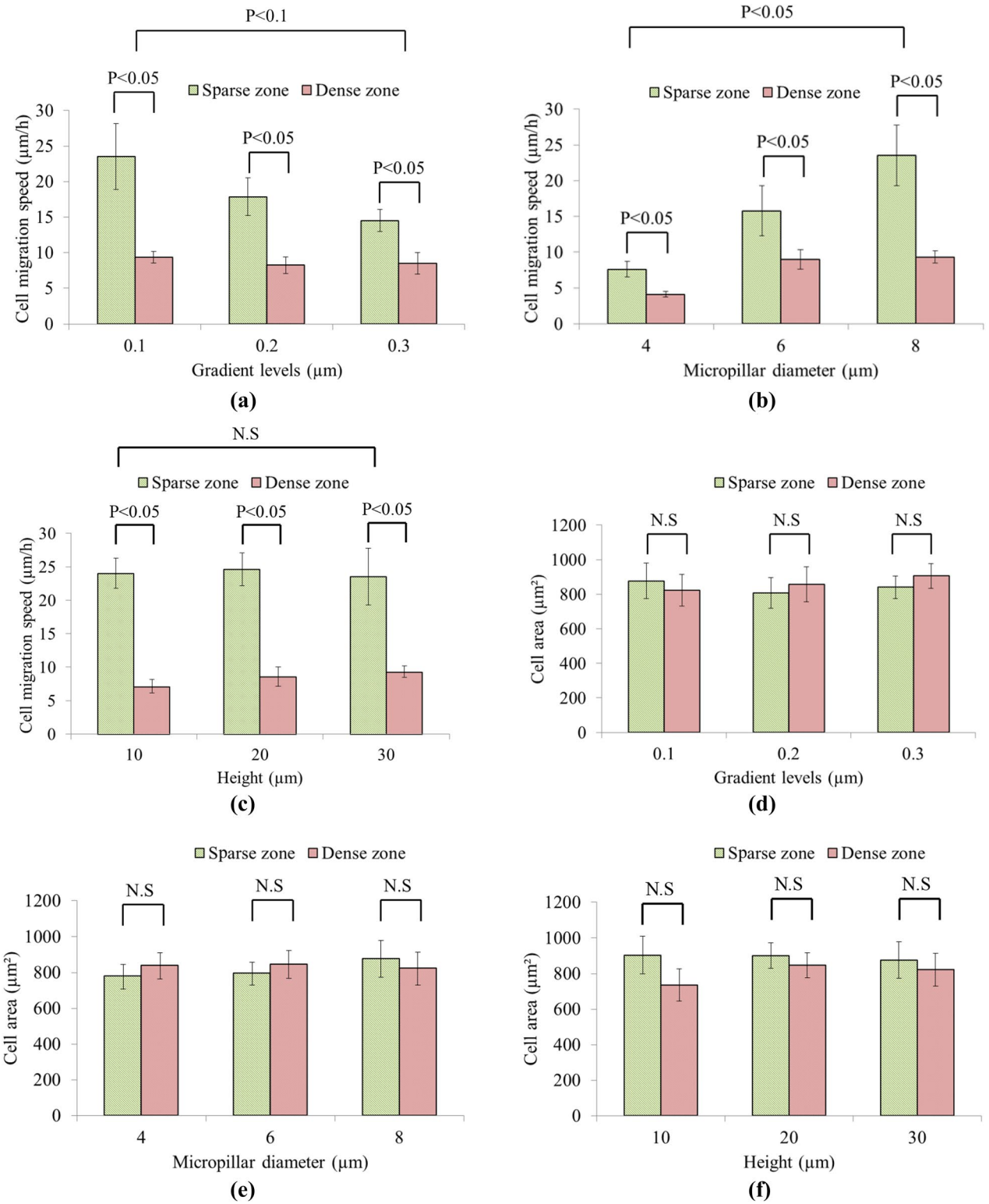

Fig. 9 Effects of three topographic parameters on cell migration: **a** effect of micropillar spacing gradient on cell migration speed, **b** effect of micropillar diameter on cell migration speed, **c** effect of micropillar height on cell migration speed, **d** effect of micropillar spacing gradient on cell spreading area, **e** effect of micropillar diameter on cell spreading area, and **f** effect of micropillar height on cell spreading area

the fibroblasts may not be able to attach the substrate very well, which may further affect the sensing of the graded topography as well as the cell migration. It is noted that the nanoscale topographic gradient was reported to successfully direct migration of cancer cells [16], which is probably due to different limits for different cell types.

During the experiments in this study, two issues were observed to significantly affect the cell migration shown in Fig. 10. In Fig. 10a, it shows that one cell was trapped between two adjacent columns of micropillars. This cell typically will not migrate along the micropillar spacing gradient direction. Instead, the trapped cell will elongate along the micropillar column direction. This phenomenon is related to topography-directed contact guidance of cells [39]. When cells are cultured on grooved surfaces, they tend to align along the direction of the grooves due to contact guidance [40]. Various cells have been demonstrated to be highly sensitive to the underlying topography of the substrate, and the presence of anisotropic cylinders has shown to influence cells to align and elongate along the stiffer direction [19]. In this study, the stiffer direction is the longitudinal direction of the micropillars because of closer distance between the adjacent micropillars. The morphology shown in Fig. 10a is similar to the reported results [40]. In this study, a gelatin layer was coated to facilitate cell attachment. Both the micropillar top and side were coated. It is observed that few cells were trapped between the micropillars. However, when investigating the effects of topographic parameters on the cell migration, majority of the cells stayed on the top of the micropillars. The few cells trapped between the micropillars were excluded. If only preferential attachment to the top of the micropillars is required, it can be achieved by only performing coating on the top of the micropillars using contact microprinting of protein on the top of the micropillars [41], and defunctionalization of the sides of the micropillars using solvents such as Pluronic F-127 [42]. In Fig. 10b, it shows more than ten cells form a cell cluster on the substrate. Inherently, the migration of single cells and the collective migration of multiple cells are biologically different processes [43, 44]. In the collective cell migration, multiple cells chemically and mechanically interact with each other and form cohesive large-scale structures. The migration speed of the collective cells is usually much smaller than the migration speed of the individual cells [15]. The cell clusters may even have a difficulty in the topography sensing [45]. The polarization of the cell cluster is dependent on the signals that are received by the cell cluster as a whole, which can result in a complex phenomenon consisting of force transmission and collective polarization [46]. In addition, the collective cell migration can also potentially degrade the underlying ECM resulting in the migration of other cells toward the cluster [47, 48]. This study focuses on the migration of individual single cells on the graded micropillar substrate. The trapped cells between the micropillars and the cell clusters are not considered when characterizing the cell polarization angle, the cell migration speed, and the cell spreading area in the previous sections.

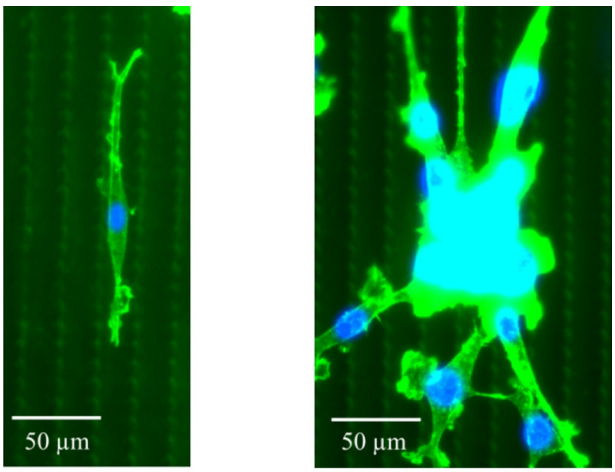

Fig. 10 Representative images of **a** cell trapped between two columns of micropillars and **b** cell cluster comprised of over ten cells. The graded micropillar substrate has a micropillar diameter of 8 μm, micropillar height of 30 μm, and spacing gradient of 0.1 μm. The green color represents the stained cell membranes, and the blue color represents the stained cell nuclei

The guided cell migration may be utilized for a variety of potential and important applications. For example, different types of cells have different stiffness and topographic sensitivity resulting in different migration behaviors. The graded micropillar substrate can be utilized for sorting of mixtures consisting of different types of cells. However, one potential issue that may arise is the reduced viability of some cell types when they are co-cultured with other cell types [49]. Another issue is that the migration of some cell types can occur preferentially toward other co-cultured cells [50], which can inhibit the separation process. Moreover, the utilization of microtextured surfaces in three-dimensional (3D) tissue constructs may enable directed cell patterning to specific locations within 3D constructs. Researchers have utilized chemical gradient-based approaches to achieve directed cell migration within 3D hydrogels [51]. The utilization of physical topographic gradients within 3D constructs provides alternative way to achieve similar directed migration without the need for additional chemicals or solvents.

Conclusions

In this paper, the graded micropillar substrate has been utilized to guide the cell migration. It has been demonstrated that the cells have been successfully guided to migrate

from the sparse zone to the dense zone. The cell polarization angle has been characterized in both sparse zone and the dense zone. Compared to the dense zone, the cells in the sparse zone are more aligned along the direction of the micropillar spacing gradient, which enables the guided cell migration. This paper further investigates the effects of the topographic parameters on the cell migration speed and cell spreading area. It is found that (1) the cell migration speed in the sparse zone decreases with the micropillar spacing gradient, increases with the micropillar diameter, and has no significant change with the micropillar height; (2) the cell migration speed in the dense zone and the cell spreading area do not change significantly under different topographic parameters; and (3) analysis of variance shows that the micropillar has the most significant effect on the migration speed in the sparse zone, and the micropillar height has the least significant effect. Future work may include investigation of the effect of micropillar shape on the guided cell migration, investigation of the effect of different cell types on the guided cell migration, and demonstration of other potential applications of the guided cell migration, such as cell separation, and directed cell patterning.

Acknowledgements This work was partially supported by Texas Tech University start-up fund and National Natural Science Foundation of China (51709120).

Compliance with ethical standards

Conflict of interest The authors declare that there is no conflict of interest.

Ethical approval This study does not contain any studies with human or animal subjects performed by any of the authors.

References

1. Lara Rodriguez L, Schneider IC (2013) Directed cell migration in multi-cue environments. Integr Biol 5(11):1306–1323
2. Painter KJ (2009) Continuous models for cell migration in tissues and applications to cell sorting via differential chemotaxis. Bull Math Biol 71(5):1117
3. Nie F-Q, Yamada M, Kobayashi J, Yamato M, Kikuchi A, Okano T (2007) On-chip cell migration assay using microfluidic channels. Biomaterials 28(27):4017–4022
4. Rennekampff H-O, Hansbrough JF, Kiessig V, Doré C, Sticherling M, Schröder J-M (2000) Bioactive interleukin-8 is expressed in wounds and enhances wound healing. J Surg Res 93(1):41–54
5. Berthier E, Surfus J, Verbsky J, Huttenlocher A, Beebe D (2010) An arrayed high-content chemotaxis assay for patient diagnosis. Integr Biol 2(11–12):630–638
6. Feng JF, Liu J, Zhang XZ, Zhang L, Jiang JY, Nolta J, Zhao M (2012) Guided migration of neural stem cells derived from human embryonic stem cells by an electric field. Stem Cells 30(2):349–355
7. Jacquemet G, Hamidi H, Ivaska J (2015) Filopodia in cell adhesion, 3D migration and cancer cell invasion. Curr Opin Cell Biol 36:23–31
8. Albuschies J, Vogel V (2013) The role of filopodia in the recognition of nanotopographies. Sci Rep 3:1658
9. Prager-Khoutorsky M, Goncharov I, Rabinkov A, Mirelman D, Geiger B, Bershadsky AD (2007) Allicin inhibits cell polarization, migration and division via its direct effect on microtubules. Cell Motil Cytoskelet 64(5):321–337
10. Devreotes P, Janetopoulos C (2003) Eukaryotic chemotaxis: distinctions between directional sensing and polarization. J Biol Chem 278(23):20445–20448
11. McCarthy JB, Furcht LT (1984) Laminin and fibronectin promote the haptotactic migration of B16 mouse melanoma cells in vitro. J Cell Biol 98(4):1474–1480
12. Lo C-M, Wang H-B, Dembo M, Wang Y-L (2000) Cell movement is guided by the rigidity of the substrate. Biophys J 79(1):144–152
13. Mycielska ME, Djamgoz MB (2004) Cellular mechanisms of direct-current electric field effects: galvanotaxis and metastatic disease. J Cell Sci 117(9):1631–1639
14. Park J, Kim D-H, Levchenko A (2018) Topotaxis: a new mechanism of directed cell migration in topographic ECM gradients. Biophys J 114(6):1257–1263
15. Kim D-H, Han K, Gupta K, Kwon KW, Suh K-Y, Levchenko A (2009) Mechanosensitivity of fibroblast cell shape and movement to anisotropic substratum topography gradients. Biomaterials 30(29):5433–5444
16. Park J, Kim D-H, Kim H-N, Wang CJ, Kwak MK, Hur E, Suh K-Y, An SS, Levchenko A (2016) Directed migration of cancer cells guided by the graded texture of the underlying matrix. Nat Mater 15(7):792
17. Hui J, Pang SW (2019) Cell migration on microposts with surface coating and confinement. Biosci Rep 39(2):BSR20181596
18. Wei J, Shi J, Wang B, Tang Y, Tu X, Roy E, Ladoux B, Chen Y (2016) Fabrication of adjacent micropillar arrays with different heights for cell studies. Microelectron Eng 158:22–25
19. Alapan Y, Younesi M, Akkus O, Gurkan UA (2016) Anisotropically stiff 3D micropillar niche induces extraordinary cell alignment and elongation. Adv Healthc Mater 5(15):1884–1892
20. Kim D-H, Provenzano PP, Smith CL, Levchenko A (2012) Matrix nanotopography as a regulator of cell function. J Cell Biol 197(3):351–360
21. Beussman KM, Rodriguez ML, Leonard A, Taparia N, Thompson CR, Sniadecki NJ (2016) Micropost arrays for measuring stem cell-derived cardiomyocyte contractility. Methods 94:43–50
22. Bayley G, Mallon P (2008) Surface studies of corona treated polydimethylsiloxane-block-polystyrene hybrid copolymer films. Polym Eng Sci 48(10):1923–1930
23. Xia W, Liu W, Cui L, Liu Y, Zhong W, Liu D, Wu J, Chua K, Cao Y (2004) Tissue engineering of cartilage with the use of chitosan-gelatin complex scaffolds. J Biomed Mater Res B Appl Biomater 71(2):373–380
24. Bodas D, Khan-Malek C (2007) Hydrophilization and hydrophobic recovery of PDMS by oxygen plasma and chemical treatment—an SEM investigation. Sens Actuators B Chem 123(1):368–373
25. Krishnamoorthy S, Noorani B, Xu C (2019) Effects of encapsulated cells on the physical–mechanical properties and microstructure of gelatin methacrylate hydrogels. Int J Mol Sci 20(20):5061
26. Wadnap S, Krishnamoorthy S, Zhang Z, Xu C (2019) Biofabrication of 3D cell-encapsulated tubular constructs using dynamic

optical projection stereolithography. J Mater Sci Mater Med 30(3):36
27. Merceron TK, Burt M, Seol Y-J, Kang H-W, Lee SJ, Yoo JJ, Atala A (2015) A 3D bioprinted complex structure for engineering the muscle–tendon unit. Biofabrication 7(3):035003
28. Ridley AJ, Schwartz MA, Burridge K, Firtel RA, Ginsberg MH, Borisy G, Parsons JT, Horwitz AR (2003) Cell migration: integrating signals from front to back. Science 302(5651):1704–1709
29. Chen Z, Li Y, Liu W, Zhang D, Zhao Y, Yuan B, Jiang X (2009) Patterning mammalian cells for modeling three types of naturally occurring cell–cell interactions. Angew Chem Int Ed 48(44):8303–8305
30. Xu H, Casillas J, Xu C (2019) Effects of printing conditions on cell distribution within microspheres during inkjet-based bioprinting. AIP Adv 9(9):095055
31. Collins T (2007) ImageJ for Microscopy. BioTechniques 43:S25–S30
32. Saez A, Buguin A, Silberzan P, Ladoux B (2005) Is the mechanical activity of epithelial cells controlled by deformations or forces? Biophys J 89(6):L52–L54
33. Ghibaudo M, Saez A, Trichet L, Xayaphoummine A, Browaeys J, Silberzan P, Buguin A, Ladoux B (2008) Traction forces and rigidity sensing regulate cell functions. Soft Matter 4(9):1836–1843
34. Wu J, Mao Z, Tan H, Han L, Ren T, Gao C (2012) Gradient biomaterials and their influences on cell migration. Interface Focus 2(3):337–355
35. Doyle AD, Wang FW, Matsumoto K, Yamada KM (2009) One-dimensional topography underlies three-dimensional fibrillar cell migration. J Cell Biol 184(4):481–490
36. Huang Y-J, Samorajski J, Kreimer R, Searson PC (2013) The influence of electric field and confinement on cell motility. PLoS ONE 8(3):e59447
37. Ponti A, Machacek M, Gupton S, Waterman-Storer C, Danuser G (2004) Two distinct actin networks drive the protrusion of migrating cells. Science 305(5691):1782–1786
38. Tremel A, Cai A, Tirtaatmadja N, Hughes BD, Stevens GW, Landman KA, O'Connor AJ (2009) Cell migration and proliferation during monolayer formation and wound healing. Chem Eng Sci 64(2):247–253
39. Crouch AS, Miller D, Luebke KJ, Hu W (2009) Correlation of anisotropic cell behaviors with topographic aspect ratio. Biomaterials 30(8):1560–1567
40. Vernon RB, Gooden MD, Lara SL, Wight TN (2005) Microgrooved fibrillar collagen membranes as scaffolds for cell support and alignment. Biomaterials 26(16):3131–3140
41. Zhu P, Tseng N-H, Xie T, Li N, Fitts-Sprague I, Peyton SR, Sun Y (2019) Biomechanical microenvironment regulates fusogenicity of breast cancer cells. ACS Biomater Sci Eng 5:3817–3827
42. Yang MT, Fu J, Wang Y-K, Desai RA, Chen CS (2011) Assaying stem cell mechanobiology on microfabricated elastomeric substrates with geometrically modulated rigidity. Nat Protoc 6(2):187–213
43. Zhang Y, Xu G, Lee RM, Zhu Z, Wu J, Liao S, Zhang G, Sun Y, Mogilner A, Losert W (2017) Collective cell migration has distinct directionality and speed dynamics. Cell Mol Life Sci 74(20):3841–3850
44. Rørth P (2009) Collective cell migration. Ann Rev Cell Dev 25:407–429
45. Trepat X, Chen Z, Jacobson K (2012) Cell migration. Compr Physiol 2(4):2369–2392
46. Trepat X, Wasserman MR, Angelini TE, Millet E, Weitz DA, Butler JP, Fredberg JJ (2009) Physical forces during collective cell migration. Nat Phys 5(6):426–430
47. Painter K (2009) Modelling cell migration strategies in the extracellular matrix. J Math Biol 58(4–5):511
48. Raeber G, Lutolf M, Hubbell J (2007) Mechanisms of 3-D migration and matrix remodeling of fibroblasts within artificial ECMs. Acta Biomater 3(5):615–629
49. Koh B, Jeon H, Kim D, Kang D, Kim KR (2019) Effect of fibroblast co-culture on the proliferation, viability and drug response of colon cancer cells. Oncol Lett 17(2):2409–2417
50. Endaya B, Guan SP, Newman JP, Huynh H, Sia KC, Chong ST, Kok CY, Chung AY, Liu BB, Hui KM (2017) Human mesenchymal stem cells preferentially migrate toward highly oncogenic human hepatocellular carcinoma cells with activated EpCAM signaling. Oncotarget 8(33):54629
51. Zhao X, Jain S, Larman HB, Gonzalez S, Irvine DJ (2005) Directed cell migration via chemoattractants released from degradable microspheres. Biomaterials 26(24):5048–5063